

## Two Kinds of Turbulence in Fluidization

Dimitri Gidaspow\*, Jonghwun Jung, Raj K. Singh and Mehmet Tartan  
Department of Chemical and Environmental Engineering  
Illinois Institute of Technology  
Chicago, IL  
[gidaspow@iit.edu](mailto:gidaspow@iit.edu)

### Abstract

*Kinetic theory based particle velocity measurements in a symmetric two-story riser show that in the core the flow is laminar and that the granular temperature is approximately given by the analogue of thermal temperature rise in Poiseuille flow. However, like in the turbulent flow in a pipe, the normal kinetic stresses are anisotropic. The shear and the normal stresses are an order of magnitude larger in riser flow than in the turbulent single phase flow. The experimental data in our two story riser agrees with newly-developed anisotropic kinetic theory. We demonstrate that turbulence of particles in a riser and in bubbling beds consists of turbulent or random oscillations of individual particles plus clusters of particles related to conventional turbulence in fluid mechanics, called Reynolds stresses. The two mechanisms of turbulence give rise to two distinct types of mixing, mixing on the level of particle scale and gross mixing on the level of bubbles or clusters containing inlet fluid. Granular temperatures for different size particles in a mixture are unequal, requiring a new kinetic theory.*

Fluidization is widely used industrially because of its continuous powder handling ability and its good heat and mass transfer characteristics. We believe these properties are due to random oscillations of nearly elastic particles. Unfortunately fluidized beds sometimes develop undesirable structures, such as large bubbles and core-annular flow. The objective of the Multiphase Fluid Dynamics Research Consortium (<http://www.mfdrc.org>) was to understand turbulence and structure of such flows.

It is well known (1, 2) that the flow regimes vary from bubbling, through turbulent, fast or circulating fluidized bed (CFB) to pneumatic transport with an increase in gas velocity. Recently the new science of computational fluid dynamics (CFD) and multiphase flow theory allowed us to compute flow and reaction in the bubbling regime (3, 1). There still exists no complete theory for the CFB regime (4, 5, 6). For developed flow the best model so far is the Jackson-Sinclair model (7) based on kinetic theory of granular flow invented by S. Savage and others (8, 2). As shown here, it does not include the observed anisotropy in the CFB regime but, at least roughly, describes the oscillations of particles that are responsible for the good mixing in the fluidized beds.

Fig.1 A shows a modified version of our earlier two-story CFB, rebuilt with a splash plate on top, to prevent the return of particles through the elbow and cause asymmetry (9). The SANDIA lab has a similar but larger riser built as a part of the Consortium whose mission was to understand riser flow. In the CFB regime a curtain of solids at the wall of the pipe restricts the use of Laser-Doppler Velocimeters for obtaining velocities in the core of the riser, vertical pipe. Hence a probe, shown in Fig.1 B was used. Fig.1 C illustrates our particle image velocity (PIV) method of obtaining instantaneous velocities,  $c$  (9). The velocity is the length of the streak divided by exposure time. The order of the colors on the rotating transparency establishes the direction. Here the study of Tartan and Gidaspow (9) is generalized to a mixture of two sizes of particles. Large particles form thicker streaks than the small particles. To obtain

radial profiles, a probe is inserted into the riser. The size of the probe was varied to establish an optimum balance between its hydrodynamic interference and sufficient number of streaks, 10 to 30, in a picture to obtain meaningful statistics of velocity averages and their variances. Fig.1 D and E show typical axial and radial velocity fluctuations of the coarse and fine particles.

Based on the experimental data a picture of riser flow has emerged. See Fig.2. In the developed flow region, there exists a laminar type core with a parabolic solids velocity profile, like Poiseuille flow. The solid line is the average velocity in the direction of flow for 530  $\mu\text{m}$  glass beads. The data for smaller particles and the data from the literature for flow of FCC particles in larger diameter pipes fall on the same universal velocity profile. The red line shows a semi-empirical correlation for the volume fraction of 530  $\mu\text{m}$  particles. It was obtained by observing that in the developed flow the solids pressure ( $P_s$ ) is constant and equal to the volume fraction of solids ( $\varepsilon_s$ ) times the granular temperature ( $\theta$ ) and particle density ( $\rho_s$ ).

Fig.3 A shows typical time average normal particle stresses in the riser computed from the definition of kinetic stresses (2).

$$\langle C_i C_i \rangle (r, t) = \frac{1}{n} \sum_{k=1}^n (c_{ik}(r, t) - v_i(r, t))(c_{ik}(r, t) - v_i(r, t)) \quad (1)$$

where  $n$  is the total number of streaks in each frame and  $C_i = c_i - v_i$ . Reference (9) shows the details of the computations. We see that the particle stresses in the direction of flow are much larger than the tangential and the radial stresses, similar to turbulent flow of gases in a pipe (12, 13), but are an order of magnitude larger. The order of magnitude of larger particle stresses for fluidization are at expense of an order of magnitude larger pressure drop. Fig.3 B shows that the laminar and turbulent shear oscillations in the core of the riser can be computed from the pressure drop minus the weight of the bed of solids, similar to the computation of the shear Reynolds stresses for a single phase flow. Such an agreement was obtained for the mixture of coarse and fine particles shown here, but not for a dilute flow of 530  $\mu\text{m}$  glass beads, except for dense flow. In a dilute flow gas turbulence is important.

Fig.4 shows the radial distribution of the dimensionless granular temperature. The granular temperature is average of normal stresses shown below.

$$\theta(r, t) = \frac{1}{3} \langle C_z C_z \rangle + \frac{1}{3} \langle C_r C_r \rangle + \frac{1}{3} \langle C_\theta C_\theta \rangle \quad (2)$$

It is dimensionalized using the mean particle velocity ( $V_m$ ), viscosity ( $\mu_s$ ) and conductivity ( $\kappa$ ). In developed flow in a riser with flow of elastic particles, the granular temperature balance (2, 7) involves a balance between conduction and generation. In cylindrical coordinates it is as follows.

$$\frac{\kappa}{r} \frac{d}{dr} \left( r \frac{d\theta}{dr} \right) = -\mu_s \left( \frac{\partial v_s}{\partial r} \right)^2 \quad (3)$$

With zero turbulent kinetic energy at the wall, the solution becomes

$$\theta = \left( \frac{\mu_s}{\kappa} \right) V_m^2 \left( 1 - \frac{r^4}{R^4} \right) \quad (4)$$

The equation is plotted in Fig.4 A. It approximately agrees with the data of 530  $\mu\text{m}$  glass beads (9). Fig.4 A also shows that the data for 156  $\mu\text{m}$  glass beads is in agreement with the solution. However, the granular temperatures for coarse and fine particles in the mixture are radically different, Fig.4 B. Fig.4 A also shows that the turbulent granular temperature is small in the core of the tube but increases toward the wall. The wall layer is dense and visually oscillating. Fig.4 A also shows that the measured granular

temperature in the two-dimensional bubbling beds agrees with the analytical solution, Equation (4). This is due to the fact that in center of the bubbling bed there is a parabolic up-flow region (14). The formation of bubbles shown in Fig.4 C also produces a bubble-like granular temperature which is higher than the granular temperature due to oscillation of particles.

The measurement of the granular temperature allows us to estimate binary diffusion coefficients,  $D$  (2). A typical value of  $D$  for the binary mixture in the core of the riser is  $106 \text{ cm}^2/\text{sec}$  obtained from the measurement of the granular temperatures. This value agrees with the diffusivity obtained by injecting  $156 \text{ }\mu\text{m}$  particles into the CFB with flow of  $530 \text{ }\mu\text{m}$  particles (15). This value is close to that reported from L.S. Fan Laboratory (16). In the bubbling fluidized beds the diffusivity measurement gives us dispersion coefficients and not the particle diffusivity. The dispersion coefficient is approximately equal to the bubble diameter times the bubble velocity.

### Acknowledgements

This study was partially supported by the National Science Foundation grant CTS 0086250 and Dow Corning via MFDRC.

### References and Notes

1. A. M. Squires, M. Kwauk, A. A. Avidan, *Science* **230**, 1329 (1985).
2. D. Gidaspow, *Multiphase flow and Fluidization* (Academic Press, San Diego, 1994).
3. M. Syamlal, T. J. O'Brien, *AIChE J.* **49**, 2793 (2003)
4. D. Gidaspow, *Recent Res. Devel. Chemical Engg.* **5**, 53 (2002 AIChE Flour-Daniel Award Lecture, 2003)
5. J. A. M. Kuipers, B. P. B. Hoomans, and W. P. M. van Swaaij, in *Fluidization IX*, L. S. Fan, T. M. Knowlton, Eds. (Engineering Foundation, New York, 1998), pp. 15-30.
6. V. Mathiesen, T. Solberg, B. H. Hjertager, *Int. J. Multiphase Flow* **26**, 387 (2000).
7. J. L. Sinclair, R. Jackson, *AIChE J.* **35**, 1473 (1989).
8. C. K. K. Lun, S. B. Savage, D. J. Jeffrey, N. Chepurniy, *J. Fluid Mech.* **140**, 233 (1984).
9. M Tartan, D. Gidaspow, *AIChE J.* **50**, 1760 (2004)
10. R. Bader, J. Findlay, T. M. Knowlton, in *Circulating Fluidized Bed Technology II*, P. Basu, J. F. Large, Eds. (Pergamon Press, New York, 1988), pp. 123-137.
11. R. Nicolai, P. M. Herbert, L. Reh, paper presented at Proc. 6th International Conference on Circulating Fluidized Beds, Winaburg, 22-27 August 1999.
12. H. T. Schlichting, *Boundary-Layer Theory* (Mc Graw Hill, New York, 1960).
13. J. Kim, P. Moin, R. Moser, *J. Fluid Mech.* **177**, 133 (1987).
14. J. Jung, PhD thesis, Illinois Institute of Technology (2003).
15. R. K. Singh, MS thesis, Illinois Institute of Technology (2003).
16. B. Du, L-S Fan, F. Wei, W. Warsito, *AIChE J.* **48**, 1896 (2002).

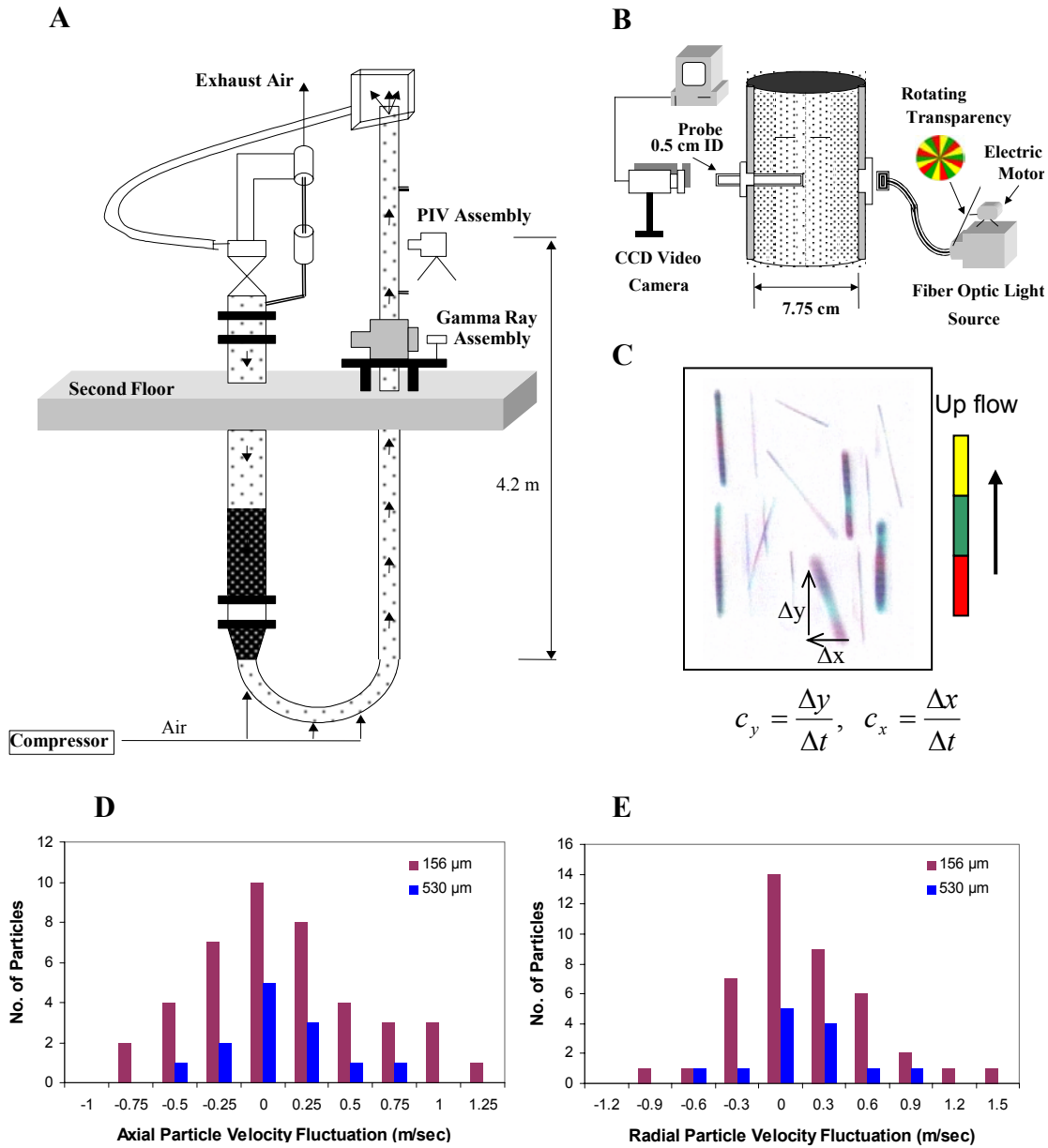


Fig.1 IIT Circulating Fluidized Bed and Particle Velocity Measurement Technique. (A) IIT circulating fluidized bed with splash plate. (B) Particle image velocity measurement system with probe. (C) Typical streak images captured by CCD camera. Thick streak line: 530 $\mu\text{m}$  glass beads, Thin streak line: 156 $\mu\text{m}$  glass beads, Exposure time: 0.0005s, Typical length: 0.1cm,  $c$ : actual velocity. (D) and (E) Typical axial and radial velocities in a mixture relative to the hydrodynamic velocity,  $(c-v)$ , where the hydrodynamic velocity  $v = \frac{1}{n} \int_{-\infty}^{\infty} cf(c)dc$ . The volume ratio of 156 $\mu\text{m}$  glass beads to 530 $\mu\text{m}$  glass beads is 3/7.  $U_g = 4.2$  m/s,  $W_{s,mix} = 14.9$  Kg/m<sup>2</sup>-s,  $\rho_s = 2460$  Kg/m<sup>3</sup>.

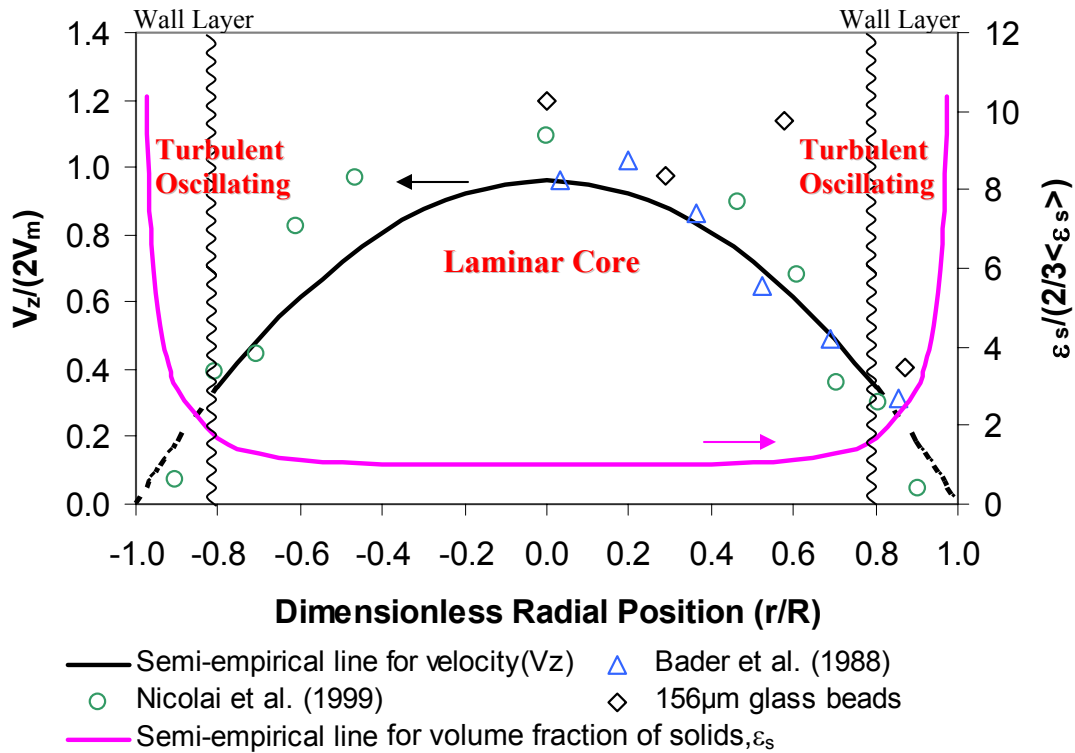


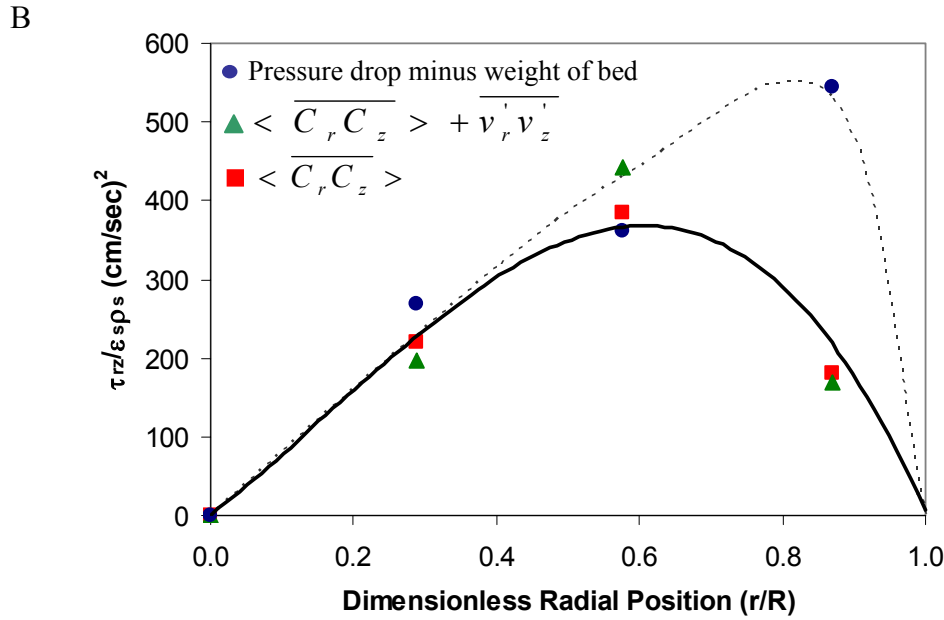
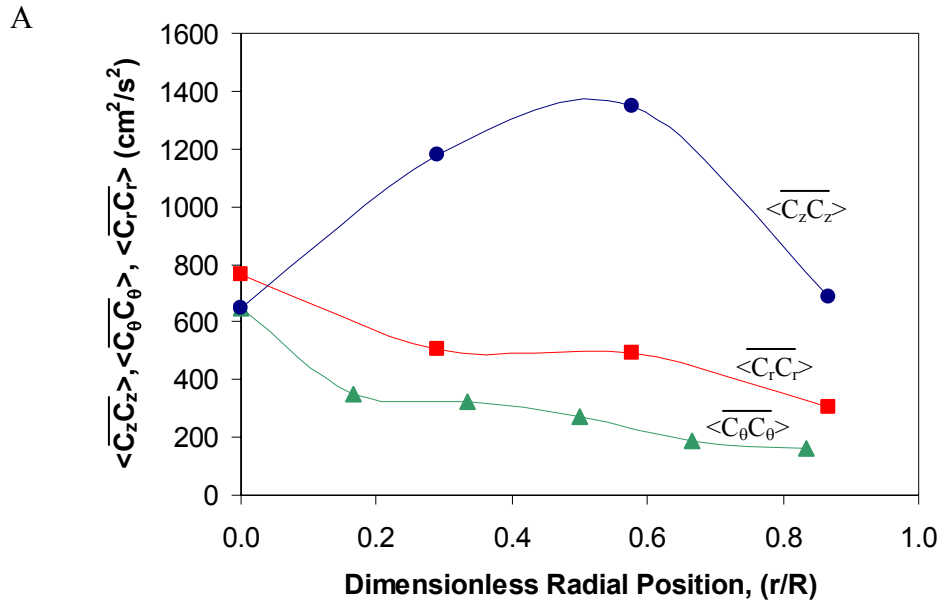
Fig.2 Flow Regime in Circulating Fluidized Beds. The semi-empirical correlations for solid axial velocity and solid volume fraction were obtained by Tartan and Gidaspow (9) with 530  $\mu$ m glass beads in the IIT riser ( $D_t = 0.076$  m).

$$V_z / (2V_m) = 0.96(1 - (r/R)^2), \quad \epsilon_s / (2/3 \langle \epsilon_s \rangle) = (1 - (r/R)^4), \quad V_m = W_s / (\epsilon_m \rho_s)$$

Bader et al. (10):  $d_p = 76 \mu\text{m}$  FCC,  $U_g = 3.7$  m/s,  $W_s = 98 \text{ Kg/m}^2\text{-s}$ ,  $D_t = 0.304$  m;

Nicolai et al. (11):  $d_p = 62 \mu\text{m}$  FCC,  $U_g = 4.3$  m/s,  $W_s = 167 \text{ Kg/m}^2\text{-s}$ ,  $D_t = 0.41$  m;

156 $\mu$ m glass beads (IIT):  $U_g = 2.65$  m/s,  $W_s = 13.3 \text{ Kg/m}^2\text{-s}$ ,  $V_m = 1$  m/s.



$$\frac{\tau_{rz}}{\epsilon_s \rho_s} = \frac{r}{2\epsilon_s \rho_s} \left( -\frac{\Delta P}{\Delta z} - \frac{2}{r^2} \int_0^r \epsilon_s \rho_s g r dr \right) = \langle \overline{C_r C_z} \rangle + \overline{v_r' v_z'}$$

Fig.3 Anisotropy and Turbulence in the IIT Riser (Similar to Turbulent Flow of Gases in a Pipe). (A) Particle normal stresses.  $d_p = 530\mu\text{m}$  Glass Beads,  $L = 4.2$  m.  $\langle \overline{C_z C_z} \rangle$  and  $\langle \overline{C_r C_r} \rangle$ :  $U_g = 5.1$  m/s,  $W_s = 14.9$  Kg/m<sup>2</sup>-s,  $\langle \overline{C_\theta C_\theta} \rangle$ :  $U_g = 4.9$  m/s,  $W_s = 14.2$  Kg/m<sup>2</sup>-s. The bar is time average. (B) Particle shear stresses in a mixture. The volume ratio of  $156\mu\text{m}$  glass beads to  $530\mu\text{m}$  glass beads is 3/7.  $U_g = 4.2$  m/s,  $W_{s,\text{mix}} = 14.9$  Kg/m<sup>2</sup>-s.

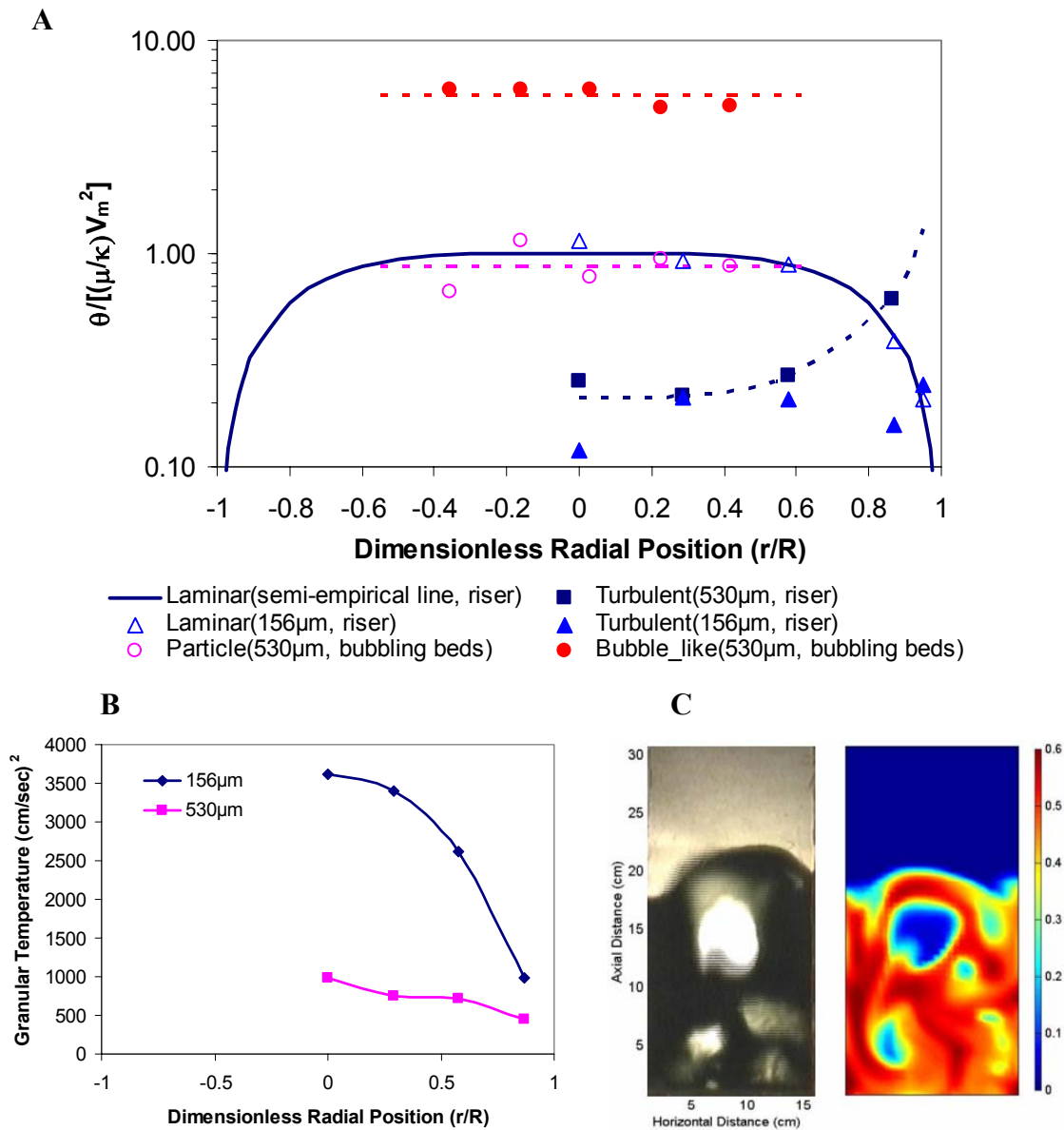


Fig.4 Turbulent Kinetic Energies ( $3/2$  Granular Temperature) in the IIT Riser and Bubbling Beds. (A) Dimensionless granular temperature,  $\theta$  scaled with mean solids velocity  $V_m$ , viscosity,  $\mu$  and conductivity,  $\kappa$  in the IIT riser ( $\mu/\kappa = 4/15, 2$ ). Riser (530 $\mu$ m):  $U_g = 5.1$  m/s,  $W_s = 21.4$  Kg/m<sup>2</sup>-s; Riser (156 $\mu$ m):  $U_g = 2.65$  m/s,  $W_s = 13.3$  Kg/m<sup>2</sup>-s,  $V_m = 1$  m/s; Bubbling Beds (530 $\mu$ m):  $U_g = 0.587$  m/s,  $V_m = 0.125$  m/s. (B) Granular temperature in a mixture in the IIT riser. The volume ratio of 156 $\mu$ m glass beads to 530 $\mu$ m glass beads is 3/7.  $U_g = 4.2$  m/s,  $W_{s,mix} = 14.9$  Kg/m<sup>2</sup>-s. (C) Typical experimental and computed bubbles in a two dimensional fluidized beds.  $d_p = 530\mu$ m glass beads,  $U_g = 0.587$  m/s.